Tidal behavior and water-level changes in gravel aquifers in response to multiple earthquakes: A case study from New Zealand

K.C. Weaver[1*], M.-L. Doan[2], S. C. Cox[3], J. Townend[1] and C. Holden[4]

[1]School of Geography, Environment and Earth Sciences, Victoria University of Wellington, PO Box 600, Wellington 6140, New Zealand

[2]Univ. Grenoble Alpes, Univ. Savoie Mont Blanc, CNRS, IRD, IFSTTAR, ISTerre, 38000 Grenoble, France

[3]GNS Science, Private Bag 1930, Dunedin, New Zealand

[4]GNS Science, PO Box 30368, Lower Hutt, Wellington, New Zealand

*Corresponding author: Konrad Weaver (Konrad.Weaver@vuw.ac.nz)

Key Points:

- Tidal behavior and water-level changes were quantified in 35 wells in response to nine earthquakes larger than M_w 5.4
- Earthquake-induced water-level and tidal behavior changes rarely occurred simultaneously in the same monitoring well (~2%)
- Permeability change thresholds correspond to peak dynamic stresses of ~0.2 to 100 kPa

This article has been accepted for publication and undergone full peer review but has not been through the copyediting, typesetting, pagination and proofreading process which may lead to differences between this version and the Version of Record. Please cite this article as doi: 10.1029/2018WR022784

Abstract

Earthquakes have been inferred to induce hydrological changes in aquifers on the basis of either changes to well water-levels or tidal behavior, but the relationship between these changes remains unclear. Here, changes in tidal behavior and water-levels are quantified using a hydrological network monitoring gravel aquifers in Canterbury, New Zealand, in response to nine earthquakes (of magnitudes M_w 5.4 to 7.8) that occurred between 2008 and 2015. Of the 161 wells analyzed, only 35 contain water-level fluctuations associated with "Earth + Ocean" (7) or "Ocean" (28) tides. Permeability reduction manifest as changes in tidal behavior and increased water-levels in the near-field of the Canterbury earthquake sequence of 2010–2011 support the hypothesis of shear-induced consolidation. However, tidal behavior and water-level changes rarely occurred simultaneously (~2%). Water-level changes that occurred with no change in tidal behavior re-equilibrated at a new post-seismic level more quickly (on timescales of ~50 minutes) than when a change in tidal behavior occurred (~240 mins to 10 days). Water-level changes were more than likely to occur above a peak dynamic stress of ~50 kPa and were more than likely to not occur below ~10 kPa. The minimum peak dynamic stress required for a tidal behavior change to occur was ~0.2 to 100 kPa.

1. Introduction

The ability of a material to transmit fluid, referred to as permeability, plays a critical role in a broad range of geological processes. In addition to its essential hydrogeological significance, permeability has in recent years been recognized as a control on hydrocarbon migration (Gluyas, 2013), the longevity of geological carbon sequestration (Gleeson & Ingebritsen, 2017), and the advection of heat and solutes in response to earthquakes (Cox et al., 2015). There is growing evidence that fluids are mechanically involved in all stages of the earthquake cycle (Sibson, 1994), and that permeability fluctuations play a key role in the rupture-reactivation-cementation cycle (e.g. Boulton et al., 2017; Dempsey et al., 2014; Sutherland et al., 2012). Permeability is considered to be dynamically self-regulating (Townend & Zoback, 2000; Weis et al., 2012), via competing processes that increase and decrease connectivity and volume of voids and fractures (Rojstaczer et al 1995). Permeability changes can be induced by earthquakes, both locally and distally, directly or indirectly through changes in static and dynamic stress (Wang & Manga, 2010).

Measurements of permeability are important in understanding tectonic and hydrogeological processes. Pumping tests are one way of estimating aquifer permeability. However, such tests represent a single point in time and space, are affected by well construction and completion, and are typically expensive. Tidal analysis, on the other hand, provides a means of estimating permeability on a continuous basis and in a non-invasive, relatively inexpensive manner (Merritt, 2004). By estimating permeability continuously, it has proven possible to detect earthquake-induced permeability changes. A pioneering study by Elkhoury et al (2006), observed earthquake-induced dynamic permeability changes with the use of groundwater-level fluctuations caused by earth tides. Many research papers have since adopted this approach (e.g. Lai et al., 2014; Liao et al., 2015; Yan et al., 2014).

Earthquake-induced water-level changes are often attributed to changes in permeability (Wang & Manga, 2010). The polarity of the water-level change (increase or decrease) in a well may be influenced by permeability changing either up or down the head-gradient of that well (Wang & Chia, 2008), with almost instantaneous responses occurring in the vicinity of the well (Shi & Wang, 2015). A higher pre-existing permeability may cause a larger water-level change and shorter decay time (Shi et al., 2013). An unresolved issue is the relationship between earthquake-induced water-level and tidal behavior changes (Elkhoury et al., 2006),

which recent studies suggest seldom occur simultaneously (e.g. Shi & Wang, 2015; Shi et al 2015; Yan et al., 2014).

Enhancement of permeability takes many forms that can involve either physical or chemical processes. The removal of colloidal blockages in heterogeneous aquifers (Brodsky et al., 2003) may alter flow pathways significantly. Fracture-scale permeability enhancement, either sub-vertical (Wang, 2007; Wang et al., 2016) or sub-horizontal (O'Brien et al., 2016), may connect hydraulically isolated pore pressure zones. Shear-induced dilation (Wang et al., 2001) may occur if cyclic shear strain exceeds $\sim 10^{-4}$ (Vucetic, 1994).

Permeability reduction is mainly documented in the interseismic environment involving chemical processes such as clay alteration (Menzies et al., 2016), fault healing (Aben et al., 2017; Gratier & Gueydan, 2007), and cementation (Dempsey et al., 2014). Co-seismic reduction of permeability has been observed in the field as a result of clogging of fractures (Shi et al., 2018; Yan et al., 2016), and can be associated with processes requiring a high level of shaking (Vucetic, 1994), notably shear-induced consolidation (Rutter et al., 2016; Wang et al., 2001) or liquefaction (Wang, 2007).

In this contribution, tidal analysis is performed on data from 161 wells in the Canterbury hydrological network, New Zealand, that have been affected by nine M_w 5.4 or larger earthquakes between 2008 and 2015. A comparison of earthquake-induced tidal behavior and water-level changes is undertaken in order to investigate the underlying processes and the scales at which they occur. An estimate of the dynamic stress perturbations required to induce changes is also calculated.

1.1 Tectonic and hydrogeological setting

Oblique collision between the Australia and Pacific plates in southwest New Zealand occurs at ~38 mm/yr (DeMets et al., 2010) and earthquakes occur throughout the country along the plate boundary zone. In the central South Island, the majority of Late Quaternary plate motion has been accommodated by slip on the Alpine Fault (Norris and Cooper, 2001). The Alpine and Marlborough faults connect two subduction zones of opposite dips: the east-dipping Puysegur trench to the south and the west-dipping Hikurangi trough to the North (Berryman et al., 1992). A damaging sequence of earthquakes in Canterbury from 2010 to 2011 was associated with distributed deformation east of the Alpine Fault (Kaiser et al., 2012; Quigley et al., 2016).

The Canterbury region is composed of Permian-Jurassic Torlesse greywacke bedrock, overlain by Paleogene-Pleistocene sedimentary sequences, and late Quaternary gravel alluvium (Brown, 2001). The gravel alluvium was sourced from tectonic uplift of the Southern Alps, and entrained and transported eastwards by glacial melt-waters (Forsyth et al., 2008). At the coast, sea-level fluctuations during glacial and inter-glacial sequences have resulted in inter-layering of fine marine and estuarine sediments with coarse-grained gravels. The finer-grained sediment thickens eastward and coastward (Brown & Weeber, 1992), forming a zone of coastal confined aquifers (Talbot et al., 1986). The coastal artesian aquifers are hydrologically heterogeneous, with laterally variable permeability and aquitard thickness (Bal, 1996). Commonly, large proportions of groundwater flow (~98%) occur through a very small proportion of the aquifers (~1%), via highly-permeable open-framework gravels (OFGs) (Dann et al., 2008).

2. Data

2.1 Seismic data

We selected nine M_w 5.4 or larger earthquakes that occurred in New Zealand between 2008 and 2015 (Figure 1); each was felt throughout the North and South islands (Table. 1). Seismic stations in the New Zealand National Seismograph Network and Strong Motion Network are operated by GeoNet (http://geonet.org.nz). In this study, we acquired seismic data for each of the nine earthquakes from broadband and strong motion seismographs. The seismic data have a sampling frequency of either 100 or 200 Hz. We applied instrument response corrections and a band-pass filter with transition bands of 0.10–0.25 Hz and 24.50–25.50 Hz. We then calculated site-specific shaking parameters as described below.

2.2 Hydrological data

Groundwater in the gravel aquifers of Canterbury is continuously monitored in 161 wells by Environment Canterbury (Figure 1). Water-levels are recorded every 15 minutes by either vented or non-vented pressure transducers. There are seven clusters of two or three wells each in which the monitoring sites contain multi-level piezometers or are in very close proximity to each other (<20 m separation). Barometric pressure sensors are distributed throughout the region and installed in monitoring well casings just below ground level. We apply barometric corrections to the non-vented pressure data so that the dataset analyzed reflects changes in water pressure only. The correction process uses barometric pressure data from the nearest site, usually within a 20 km distance and 300 m elevation of the respective well.

Sea-level monitoring in the Canterbury region is undertaken by The National Institute for Water and Atmospheric Research (NIWA). These sites are located in Christchurch, and Timaru (Figure 1; see Supplementary data). Data are recorded at 15 minute intervals by pressure transducers and provide information on the time and amplitude of ocean tide fluctuation.

3. Materials and methods

3.1 Tidal computation

We quantify the responses of aquifers to tidal strains predicted from astronomical laws in order to model the temporal evolution of hydraulic and poroelastic parameters (Bower & Heaton, 1978; Bredehoeft, 1967; Hsieh et al., 1987). The gravitational effects on the Earth of celestial bodies induce Earth deformation and produce tidal potential energies. The resulting tidal potential spectrum (W) is the sum of a large number of components (k):

$$W = \sum_{k} W_k \tag{1}$$

The combination of solar and lunar forcing produces two main groups of components, diurnal (1 cycle per day; 1 cpd) and semi-diurnal (2 cpd): O_1 (0.9295 cpd); S_1 (1 cpd); K_1 (1.0027 cpd); M_2 (1.9323 cpd); S_2 (2 cpd); and K_2 (2.0055 cpd) (Wilhelm et al., 1997). Each tidal potential component (W_k) has a corresponding frequency (ω_k) and can be expressed with respect to complex coefficients (a_k):

$$W_k = a_k e^{i\omega_k t} \tag{2}$$

Frequency-domain analysis enables different components of the tidal spectrum to be identified in water-level time-series from monitoring wells (see Supplementary data). Wells exhibiting water-level fluctuations caused pre-dominantly by S_1, S_2, K_1 or K_2 tend to be

dominated by barometric and thermal effects (Doan et al., 2006). Water-level fluctuations caused by all but the M_2 and O_1 components are sensitive to thermal and anthropogenic disturbances. Typical amplitudes of the M_2 component are larger than those of the O_1 component (Wilhelm et al., 1997). Also the sea-level sites in Canterbury exhibit a larger ocean tide amplitude of the M_2 component ($\sim$763 mm) than the O_1 ($\sim$28 mm) component (see Supplementary data). As a result, only water-level fluctuations caused by the M_2 component were considered in the analysis.

We have used the software package Baytap08, modified for application to high-frequency data, to decompose the observed water-level data (h) into constituent tidal signals (h_k). Baytap08 uses a time-domain Bayesian modelling procedure (Tamura and Agnew, 2008) to estimate a series of complex coefficients ($c_k = A_k e^{i\phi_{lag}}$) such that

$$h = \sum_k h_k = \sum_k c_k . \frac{W_k}{gR} \tag{3}$$

with gravitational acceleration ($g, 9.81\ m/s^2$) and radius of the Earth ($R, \sim 6371$ km). The c_k coefficients are related to the expected poroelastic response of the aquifer relative to the tidal strain. For each tidal component, in the first-order geometrical representation of the Earth, there is a volumetric strain contribution (δ_k) (Doan et al., 2006)

$$\delta_k = \frac{1-2\nu}{1-\nu}[2l - 6s]\frac{W_k}{gR} \tag{4}$$

that depends on Love ($l, 0.606$) and Shida parameters ($s, 0.0840$). Of the rock types for which poroelastic moduli have been systematically collated (Wang, 2000), down-scaled in the laboratory environment, sandstone appears to be the most comparable to the Canterbury gravel aquifers at depth, in both poroelastic and architectural (sedimentary facies) terms. Therefore, we assume the average of the Poisson's ratio for sandstones compiled by Wang (2000) to represent the Canterbury gravel aquifers at depth ($\nu, 0.3$). In an undrained porous medium, a change in strain (δ) would induce a change in pore pressure, $p = BK_u\delta$ governed by Skempton's coefficient (B, dimensionless) and the undrained bulk modulus (K_u, GPa). As $p_k = \rho g h_k$,

$$c_k = \frac{\frac{1-2\nu}{1-\nu}[2l-6s]}{\rho g} BK_u \tag{5}$$

We refer to the term BKu as an apparent BKu, as we assumed here that the tidal variations in pore pressure were dominated by the poroelastic response to tides. If this assumption is wrong, the computed value of BKu would exceed poroelastic predictions and not be representative.

3.2 Water-level fluctuations caused by earth and ocean tides

The tides that cause water-level fluctuations in wells analyzed here have two origins, which we consider below: (1) the poroelastic response to strain induced by earth tides, and (2) the effect of ocean tides via pore pressure diffusion throughout the aquifer or direct mechanical loading.

Tidal loading imposes volumetric strain on the Earth (Agnew, 2005). The resultant dilation and contraction of the Earth causes pore pressure variations throughout groundwater aquifers. However, for shallow unconfined aquifers, this pore pressure fluctuation may be rapidly dissipated by vertical pore pressure diffusion to the surface (Roeloffs, 1996).

Solar and lunar gravitational loading also produces water level fluctuations in the ocean, the oceanic tides (Merritt, 2004). Whereas the hydraulic response to earth tides is typically of the scale of several tens of centimeters, the amplitudes of oceanic tides can exceed several meters. Ocean tides can induce direct mechanical loading at the coast. Software like SPOTL (Agnew, 2012) predicts this mechanical loading from global or regional models of oceanic tides. If ocean tidal gauge time-series data are available, the loading can by analytically computed from the Boussinesq equation (Doan, 2005). Pressure changes associated with ocean tides can also diffuse inland by direct hydraulic connection between the ocean and coastal aquifers. This induces water-level fluctuations in wells (Ferris, 1951). Analytical solutions (Van der Kamp, 1972) show that oceanic tides can in some situations propagate tens of kilometers inland (Merritt, 2004).

There are three states of coupling between monitoring wells and aquifers that control the recording of pore pressure variations in wells caused by earth and ocean tides in aquifers (Doan, 2005; Hsieh et al., 1987):

1) Coupled — Permeability is large and/or pore pressure fluctuations are slow, so that the water-levels in monitoring wells perfectly correlate with pore pressure variations in aquifers.
2) Uncoupled — Permeability is small and/or pore pressure fluctuations are rapid so that the pore pressure variations in aquifers are not observed in monitoring wells.
3) Transitional — In an intermediate case, the water-levels in monitoring wells partly reflect the pore pressures in aquifers. The phase lag (ϕ_{lag}) describes the partial coupling and is dependent on the hydraulic properties around each monitoring well. In this case, aquifer properties can be monitored.

There are also cases in which both earth and ocean tides contribute to water-level fluctuations in monitoring wells (e.g. Doan, 2005) and numerous aquifer configurations and tidal models with respect to coastal aquifers have been proposed (Merrit, 2004). These include: an aquifer and overlying confining layers cropping out at or near the coastline (Jacob, 1950; Ferris, 1951); a completely confined aquifer extending under the sea (Van der Kamp, 1972); and a leaky contained aquifer system extending under the sea for a distance (Li and Jiao, 2001). Therefore, distinguishing between the effects of earth and ocean tides is not entirely unique, as the expected amplitudes are dependent on individual site conditions. Here, a quantitative assessment was adopted to distinguish between monitoring well water-level fluctuations resulting from a combination of earth and ocean tides ("Earth + Ocean"), from ocean tides ("Ocean"), and other non-tidal processes ("No tide"):

1) The first criterion was based on the raw amplitude of the M_2 component, which differentiated between the tidally-sensitive and tidally-insensitive wells. Any wells with a tidal M_2 amplitude of <1 mm were classified as having no tides, as the fluctuations were smaller than the measurement uncertainties. Furthermore, wells exhibiting fluctuations caused pre-dominantly by S_1, S_2, K_1, or K_2 were classified as being contaminated by non-tidal effects.
2) The second criterion was based on the magnitude of the apparent BKu, considering only those wells already classified as tidally-sensitive using the first criterion. Sandstone is the most comparable lithology in both poroelastic and architectural (sedimentary facies) terms with the Canterbury Plains aquifer system, and thus the arithmetic mean of sandstone BKu values was computed from eight previously published measurements (12 GPa; Wang, 2000). The arithmetic mean was taken as the maximum acceptable BKu for the Canterbury Plains aquifer system as the wells

studied penetrate a range of different lithologies from gravels to sandstones with varying degrees of compaction. The maximum acceptable BKu value was only used to discriminate between wells containing fluctuations associated with (1) Earth + Ocean and (2) Ocean tides. Water-levels that pre-dominantly responded poroelastically to tides have an apparent BKu <12 GPa (Earth + Ocean tides). When apparent BKu exceeds 12 GPa, water-levels most likely responded to Ocean tides as the apparent BKu exceeds poroelastic predictions. Pressure-meter tests were not deemed suitable for the assessment of poroelastic moduli as interpretation methods can lead to large differences in parameters obtained (Mair and Wood, 2013).

3) A qualitative assessment of the water-level fluctuations also assisted classification: Earth + Ocean tide fluctuations contain proportionately larger O_1 amplitudes than M_2 amplitudes, compared to Ocean tide fluctuations (see Supplementary data).

3.3 Earthquake-induced tidal behavior changes

The phase lag (ϕ_{lag}), was computed in 30-day windows shifted in 7.5 day increments. The 30-day window analysis was applied to 10 separate time intervals between January 2008 and January 2015. Each of the 10 analyses corresponds to an inter-seismic period (Table 1). The tidal analyses started one day after and stopped one day before each earthquake. The times of the earthquakes were never included in the analyses, to avoid abnormal water-level changes adversely affecting the calculation of tidal effects. The phase lag is generally negative and should range between –80 and 0 degrees (Hsieh et al., 1987). However, positive phase lags can occur for various reasons: ocean tides; anisotropy (fracture orientation (Bower, 1983)); lateral boundaries; and changes in topography (e.g. Harrisson, 1976). Attenuation of tidal amplitude and decreases in phase lag also occur with decreased confinement and increased leakage (Roeloffs, 1996). In this study, ϕ_{lag} decreases and ϕ_{lag} increases have been interpreted as horizontal permeability increases and decreases respectively, as in previous studies (Elkhoury et al., 2006; Roeloffs et al., 2003; Xue et al., 2013). We do not constrain the true phase lag values with more sophisticated models of the wells and aquifers, as this study is not well-specific, and pumping tests and bore logs are not readily available. This is a multi-site, multi-earthquake study that investigates the absolute change in phase lag induced by earthquakes.

3.4 Earthquake-induced water-level changes

Earthquake-induced water-level changes can be separated into co-seismic and post-seismic components. Some previous studies have defined water-level changes during and after earthquake shaking as purely co-seismic (e.g. Shi et al., 2015b) while others use the term co-seismic even when groundwater is sampled hourly (e.g. Wang et al., 2004). To avoid confusion, in this study we have defined co-seismic as water-level changes that occur during earthquake shaking and post-seismic as water-level changes that occur after earthquake shaking has ceased. Since monitoring well water-levels were sampled every quarter-hour, the observed changes were all considered post-seismic and not co-seismic. The amplitude, polarity and duration of these post-seismic water-level changes were recorded. Water-level changes were also classified as either transient (returning to pre-earthquake levels within two hours) or persistent (lasting several days).

To perform a systematic comparison between water-levels and tidal behavior changes, the comparison must take place on a similar time-scale of response, as the longevity of the response is partly determined by the processes by which they are induced. As the tidal behavior changes described here were observed over 7.5-day staggered increments in 30-day windows (a minimal analysis duration to ensure good separation between the M_2 and S_2 tidal

components), only persistent water-level changes have been examined. A series of short earthquake-induced fluctuations that returned to background levels within two hours are termed transient and recorded as "no change" as they represent transitory changes which tidal analysis was unable to detect.

3.5 Stress changes

Earthquake-induced stress changes can be of static or dynamic character, and exhibit different characteristic decreases with distance from the earthquake (Manga & Brodsky, 2006). The distance r from the epicenter is often categorized as follows: near-field representing distances within ~one ruptured fault length, far-field representing distances multiple times greater than the fault length, and intermediate-field for distances in between (Wang & Manga, 2010). Static stress changes decay at $\sim 1/r^3$ and are most significant in the near-field (Lay & Wallace, 1995; Manga & Wang, 2007). Dynamic stress changes are of a higher magnitude than static stress changes and decrease in proportion to $\sim 1/r^{1.66}$ (Lay & Wallace, 1995). In other words, dynamic stress changes dominate at intermediate to far-field distances (Wang & Manga, 2010).

Wakita (1975) proposed that persistent water-level responses reflect earthquake-induced static strain perturbations, a result reinforced by subsequent studies (Akita & Matsumoto, 2004; Chia et al., 2008; Jónsson et al., 2003; Quilty & Roeloffs, 1997; Roeloffs, 1996). However, the magnitude of water-level responses in the intermediate- and far-field are often larger than predicted by poroelastic theory (Manga & Wang, 2007). The spatial distribution of hydrological responses induced by the Darfield earthquake (~55 km average distance), is inconsistent with static stress change calculations (Zhan et al., 2011) and has been interpreted as a consequence of dynamic stresses (Cox et al., 2012, Rutter et al., 2016). Most of the wells considered here are in the intermediate- or far-field with respect to the earthquake sources and therefore only dynamic stress changes have been considered. The peak dynamic stress change (PDS, GPa) were calculated (Jaeger & Cook, 1979):

$$\mathrm{PDS} \sim \frac{\mu_S \mathrm{PGV}}{v_s} \tag{7}$$

with maximum peak ground velocity (PGV, $\mathrm{m/s}$), shear modulus (μ_S, GPa) and shear-wave velocity at the monitoring well ($v_s, \mathrm{m/s}$). In this study, maximum PGV was calculated at seismic stations and interpolated to wells using the nearest neighbor method (Ebdon, 1984). The small-strain shear modulus is a function of the void ratio and the effective mean confining stress (Clayton, 2011; Hardin and Drnevich, 1972). Although the shear modulus is influenced by the gravel content, the shear modulus only varies by ±0.2 MPa. Considering the monitoring wells are generally shallow (<100 m), a shear modulus value of 0.14 GPa was used, an arithmetic mean of the small-strain shear modulus for unconsolidated gravels (Chen et al., 2018). Shear-wave velocities were based on geological site classifications (Horspool et al., 2015). Uncertainties in shear-wave velocity (±30 m/s), peak ground velocity (±1 mm/sec), shear modulus (±4 GPa), and the simple relationship employed for estimating PDS, require us to use PDS only as an approximation, as uncertainties can exceed ~10% of the calculated values.

3.6 Uncertainties and assumptions

Tidal behavior and water-level changes were observed after notable earthquakes, and it is assumed that the largest-magnitude event was the cause of the perturbation. There is a possibility, however, that perturbations could alternatively have been produced or enhanced by smaller-magnitude aftershocks or near-field earthquakes. In this study, secondary events are assumed not to induce hydrological changes.

Attempts have been made elsewhere to assess the potential for tidal behavior and water-level changes to reflect precursory seismic processes (Liu et al., 2013). Considering the heterogeneity of the Canterbury aquifer system (Dann et al., 2008), seasonal changes in hydraulic head are expected to cause a deviation in mechanical and hydraulic properties (Miller & Shirzaei, 2015). With such variability, small precursory earthquake signals are unlikely to be detected, even if present, and these have been ignored.

Many wells incurred damage as a result of the Canterbury earthquake sequence. The elevation of several monitoring well heads changed as a result of the buoyant rise of casing and/or ground subsidence, which affected the measurement of water levels and necessitated re-surveying. Elsewhere, damaged logging equipment and screens were replaced and re-pumped. New elevations are used here for boreholes where re-surveying had been completed, otherwise it was assumed any anthropogenic influence on the data or data-quality were minor or easily identified and corrected for.

Absolute ground-water levels are generally known to ±50 cm relative to sea-level, once corrected for barometric pressure variations and surveying uncertainties. Relative ground-water level changes are known much more precisely, with changes induced by earthquakes and or tides occurring on scales of ±1 cm.

4. Results

4.1 Identification of the origin of the tides

Water-level fluctuations caused by earth and ocean tides contain similar components of the tidal spectrum, despite different processes causing them. It is important to identify water-level fluctuations caused by earth and ocean tides and to determine which phenomenon is predominantly responsible. The maximum acceptable BKu value (12 GPa) that was used to discriminate between (1) Earth + Ocean and (2) Ocean tides did not affect the results, data analysed or findings if varied.

Earth + Ocean tide monitoring wells generally occur far from the shore and reach depths exceeding 60 m, whereas monitoring wells containing a Ocean tides are generally close to the shore (within 6 km of the coast) and of shallow depths (Figure 2, 3 & 4). The water-level fluctuations caused by Ocean tides had amplitudes of up to 460 mm, significantly larger than those of water-level fluctuations caused by Earth + Ocean tides (<19 mm). The water-level fluctuations caused by Ocean tides were of the same order of magnitude as the sea-level gauge amplitude (~763 mm, see Supplementary data). Monitoring wells insensitive to tides may be too shallow to be influenced by earth or ocean tides (Figure 2 & 3).

Of the 161 wells, only 35 (22%) were considered sensitive to tides (Figure 2). Of the 35 wells sensitive to tides, seven (~4% of the original wells) are sensitive to Earth + Ocean tides, and 28 (~17%) sensitive to Ocean tides.

4.2 Earthquake-induced changes in tidal behavior

We focus on the temporal evolution of the tide-sensitive wells by analyzing changes in the M_2 ϕ_{lag} induced in these wells by any of the nine earthquakes studied (Table 2). The M_2 ϕ_{lag} was compared in the inter-seismic period before and after each earthquake (Figure 5). If the absolute change in M_2 ϕ_{lag} spanning each earthquake was larger than the natural variations in M_2 ϕ_{lag}, the polarity and amplitude of change were recorded.

In the 35 monitoring wells, nine responses to earthquakes in M_2 ϕ_{lag} occurred. Earthquake-induced tidal behavior changes occurred as a result of the Darfield (M_w 7.1), Christchurch (M_w 6.2, 6.0, 5.9) and Opunake (M_w 6.2) earthquakes. There were seven cases of ϕ_{lag}

decreasing and two cases of ϕ_{lag} increasing. The largest ϕ_{lag} increase was 26° and the largest ϕ_{lag} decrease was 57°. M_2 ϕ_{lag} change occurred four times in only one monitoring well that displayed Earth + Ocean tides: H39/0148 (Figure 5 & 6). The lowest peak dynamic stress (PDS) required for an Earth + Ocean tide behavior change in H39/0148 was ~0.2 kPa (Figure 7). M_2 ϕ_{lag} change occurred five times in monitoring wells that displayed Ocean tides. The five changes occurred once in three wells and twice in one well (Figure 6). In H39/0148, which has a large seasonal variation in hydraulic head (Figure 5e), tidal behavior may be influenced by changes in boundary conditions. The lowest PDS required for an Ocean tide behavior change was ~2 kPa. In the clustered wells sub-set, only two wells responded to an earthquake with a tidal behavior change (Figure 6). There is no clear statistical difference between no tidal behavior change and tidal behavior change, based on PDS, in these gravel aquifers (Figure 7).

4.3 Earthquake-induced water-level changes

Within the 161 wells monitored during the nine earthquakes, there were a total of 203 water-level changes, with 122 increases and 81 decreases (Table 3). The water-level changes ranged from −94 to 240 cm. The Hastings (M_w 5.4) earthquake did not produce persistent changes (Table 3). The different earthquakes generally produced water-level changes of different polarities in each monitoring well. A water-level change occurred in ~38% (Earth + Ocean tide subset), ~22% (Ocean tide subset) and ~19% (No tide subset) of instances (Figure 7). In the Earth + Ocean and Ocean tide subsets, the maximum number of changes observed in an individual well was four times. Nine wells had no response to any of the nine earthquakes. In the individual well clusters, in the rare case that water-level changes occurred in all wells in response to a particular earthquake, water-level change polarity was inconsistent (Figure 6). Below a peak dynamic stress of ~10 kPa, it is more than likely that no water-level change will occur. Above ~50 kPa, it is more than likely that a water-level change will occur. Between ~10 kPa and ~50 kPa, there is a transition from no water-level change to a water-level change (Figure 7). An increased sensitivity to rainfall after the February 2011 earthquake in M36/7535 (Figure 5c) may suggest a change in the level of confinement.

4.4 Comparison of tidal behavior and water-level changes

For the most part, tidal behavior and water-level changes occurred independently (Figure 8). There were four tidal behavior changes, and 53 water-level changes that occurred independently. Only in four cases did tidal behavior and water-level changes occur simultaneously. Of these four cases, two included a ϕ_{lag} decrease and two included a ϕ_{lag} increase (Table 4). In the well clusters, only one tidal behavior change occurred with an accompanying water-level change (M36/5384, Darfield earthquake; Figure 6). In most other cases, water-level changes occurred independently either in one or two wells within each cluster. Water-level changes that occurred without tidal behavior changes, generally equilibrated sooner (~50 mins) than those with tidal behavior changes (~240 mins to ~10 days) (Figure 9).

5. Discussion

5.1 Mechanisms for earthquake-induced water-level and tidal behavior change

Numerous mechanisms may cause changes in water-level and tidal behavior following earthquakes. Shear-induced dilation in unconsolidated deposits (Wang et al., 2001) occurs when cyclic shear strains exceed a threshold of ~10^{-4} (Luong, 1980). An increase in porosity, and a decrease in pore pressure leads to consistent earthquake induced water-level decreases (Wang & Chia, 2008). At a lower cyclic shear strain, but still exceeding ~10^{-4} (Dobry et al.,

1982, Vucetic, 1994), shear-induced consolidation and liquefaction occurs (Wang et al., 2001, Wang, 2007), resulting in consistent earthquake induced water-level increases (Wang & Chia, 2008). In this study, the Canterbury earthquakes of 2010 and 2011 induced seismic shaking that exceeded the seismic energy density threshold for liquefaction (~0.1 J/m^3; Wang et al., 2006), at the majority of monitoring wells. The 2010 M_w 7.1 Darfield and the 2011 M_w 6.3 Christchurch earthquake both induced tidal behavior changes in two separate monitoring wells, probably related to a decrease in permeability. A simultaneous increase in water-level was observed at these wells. Furthermore, the 2010 M_w 7.1 Darfield earthquake induced post-seismic persistent water-level increases in the near-field (see Supplementary data). These observations are consistent with reductions in permeability measured by step-drawdown tests in the vicinity of the Darfield epicenter, three years after the event (Rutter et al., 2016), and shear-induced consolidation.

High levels of seismic shaking can also cause breaching of aquitards and enhancement of vertical permeability (Wang et al., 2016). As the Canterbury aquifer system at depth is artesian, any enhancement of vertical permeability would result in the upward movement of groundwater. The 2010 M_w 7.1 Darfield and the 2011 M_w 6.3 Christchurch earthquakes induced water-level decreases in confined aquifers and water-level increases in unconfined aquifers, indicative of upward movement of groundwater (Gulley et al., 2013). In Taiwan, Wang et al (2016) studied clustered well responses to the 1999 M_w 7.6 Chi-Chi earthquake and interpreted the convergence of water-levels in stratified aquifers and post-seismic phase response similarity in confined and unconfined aquifers to be evidence of the vertical enhancement of permeability and upward movement of groundwater. In the seven clusters studied here, water-level changes occurred independently most of the time. Only two instances of tidal behavior change occurred, one decrease in permeability (above the liquefaction threshold) and one increase in permeability in the intermediate-field in response to the 2012 M_w 6.2 Opunake earthquake. The clustered wells in the data-set studied here show no substantial evidence for enhancement of vertical permeability. Unfortunately, monitoring wells with earth and/or ocean tides in the Canterbury Plains are scarce, and thus significantly reduce the data-set for assessing this hypothesis.

At lower levels of shaking, horizontal permeability can be enhanced or reduced by the re-distribution of colloidal particles. Seismically induced groundwater flow velocities (Wang et al., 2009) have the potential to dislodge colloids from flow pathways and enhance permeability (Brodsky et al., 2003; Matsumoto et al., 2003; Wang & Chia, 2008). Seismic shaking may also mobilize sediment that further blocks these flow pathways (Rutter et al., 2016). The dislodging of colloids may result in random polarity of resultant water-level changes (Wang & Chia, 2008). Controlled experiments of pore unclogging (Elkhoury et al., 2011; Liu & Manga, 2009) and earthquake-induced groundwater color changes (Prior & Lohmann, 2003) support the hypothesis of permeability enhancement via colloidal dislodgement. Considering the Canterbury gravel aquifer system is made up of highly permeable open framework gravels that accommodate ~98% of flow through ~1% of the aquifer (Dann et al., 2008), it is perhaps possible to induce substantial permeability change by colloidal re-distribution in preferential flow pathways. Such changes could also occur in the immediate surroundings of a monitoring well (Shi et al., 2015a) or at flow boundaries. Water-level changes, both increases and decreases, and tidal changes which occurred below the liquefaction threshold may have resulted from colloidal re-distribution, either enhancing or reducing permeability.

5.2 Peak dynamic stress

We compare the peak dynamic stress (PDS) required to induce water-level and tidal behavior changes in the Canterbury gravel aquifers. Permeability reduction detected by tidal behavior changes produced by the 2010 M_w 7.1 Darfield and the 2011 M_w 6.3 Christchurch earthquake required a PDS of ~200 kPa. The permeability reduction coupled with post-seismic water-level increases, we suspect, is a result of shear-induced consolidation which requires a high level of shaking (Vucetic, 1994).

The minimum PDS required for permeability increases in the Canterbury gravel aquifers is ~0.2 to 100 kPa (Figure 7). However, owing to a small number of tidal responses recorded, there is no clear distinction between the presence and absence of tidal behavior changes based on PDS. Water-level changes are more than likely to occur in response to peak dynamic stresses above ~50 kPa and more than likely to not occur below ~10 kPa (Figure 7).

Although the hypotheses above may provide explanations for the water-level and tidal behavior changes observed, in the vast majority of instances monitoring wells that experienced a PDS of between ~10^{-1} and 10^3 kPa did not respond to the earthquakes with persistent tidal behavior and/or water-level changes. The monitoring wells that didn't respond may be screened in aquifers that have high storage capacities or poor permeability. This in-turn may result in a higher shaking threshold required for a change to be observed as the monitoring well and aquifer are uncoupled (Doan et al., 2006; Hsieh et al., 1987). The low bulk modulus of unconsolidated gravels may also contribute to monitoring wells not responding with water-level or tidal behavior changes (Roeloffs, 1998). Other shaking (source factors) and/or hydrogeological (receptor factors) parameters may also control the threshold for tidal behavior and water-level changes.

5.3 Comparison of tidal behavior and water-level changes

The results here show significant inconsistency between tidal behavior and water-level changes. Only ~2% of the cases observed had a water-level change coincident with a tidal behavior change (cf. 33%, Shi et al., 2015a; 43%, Yan et al., 2014). Water-level changes that occurred without tidal behavior changes took a median of ~50 minutes to re-equilibrate at the new post-seismic water-level (Figure 9). The fast re-equilibration time may be a result of high permeability and good coupling between the monitoring well and aquifer (Doan et al., 2006, Hsieh et al., 1987). Furthermore, the water-level changes may have returned to pre-earthquake levels sooner than 30 days after the earthquake, possibly resulting in no small tidal behavior change being detected. Tidal changes may also not have been observed in these cases, possibly due to the unconsolidated gravels having a relatively low bulk modulus (Roeloffs, 1998) and thus being less sensitive to tidal behavior changes than other rock types. It should also be considered that these water-level changes may represent permeability changes in the local surroundings, producing the short re-equilibration times. The small-scale (m) nature of these permeability changes may be too small to alter tidal behavior (Shi et al., 2015a).

In each monitoring well, the different earthquakes generally produced water-level changes of different polarities, which is in contrast with some previous observations (e.g. Roeloffs, 1998; Wang and Chia, 2008). This is not surprising, however, considering the variety in shaking amplitude, duration, and frequency experienced across the earthquake intervals. Monitoring wells were not consistently in the near- or intermediate-field for the data-set, and thus were subject to variable shaking intensities. Furthermore, aquifer susceptibility to earthquake-induced process may have changed with each successive earthquake (Elkhoury et al., 2006; Xue et al., 2013), although there does not appear to be any significant change in ground strength following the Canterbury earthquake sequence (Lees et al., 2015; Orense et al., 2012).

Water-level changes that occurred with tidal behavior changes took from ~240 mins to ~10 days to re-equilibrate at the new post-seismic water-level (Figure 9). The re-equilibration time was larger than for independent water-level changes. Tidal behavior changes indicated an equal number of permeability increases and decreases. These water-level and tidal behavior changes may reflect transitional coupling between the monitoring well and the aquifer due to lower permeability (Doan et al., 2006, Hsieh et al., 1987). The permeability changes may occur on a larger scale than permeability changes detected by independent water-level changes, as water-level changes also occurred in nearby wells where present.

There are instances in which tidal behavior changes occurred without water-level changes, requiring a different explanation. We hypothesize that low permeability resulted in an uncoupled state between monitoring wells and aquifers. Under these conditions, permeability changes in aquifers might not be observed in monitoring wells on the time-scale that water-level changes are identified (days), but may still be detected on the time-scale of tidal behavior changes (30 days). Low signal to noise ratios may also have prevented water-level changes being recorded.

6. Conclusion

(1) In the near-field of the Canterbury earthquake sequence of 2010 and 2011, permeability reduction and increased water-levels support the hypothesis of shear-induced consolidation. The hydrological responses to the earthquakes north and south of Canterbury included variable water-level change polarities and rare tidal behavior changes, suggesting permeability enhancement or reduction in the local aquifer.

(2) Water-level changes that occurred without tidal behavior changes took ~50 minutes to re-equilibrate at a new post-seismic water-level, while those that occurred with tidal behavior changes took from ~240 minutes to ~10 days to re-equilibrate. The fast re-equilibration time of independent water-level changes may be due to a high permeability and good coupling between the well and the aquifer, and/or small permeability changes in the local aquifer. Tidal behavior changes may have also not been observed due to the low bulk modulus of the gravels. Water-level changes that occurred with tidal behavior changes may occur on a larger scale than independent water-level changes, as water-level changes also occurred in nearby wells where present.

(3) The minimum peak dynamic stress required for a tidal behavior change in the Canterbury gravel aquifers was ~0.2 to 100 kPa. Water-level changes were more than likely to occur above ~50 kPa and were more than likely to not occur below ~10 kPa. However, there was no clear distinction between the presence and absence of tidal behavior and water-level changes based on peak dynamic stress.

Acknowledgments

This study was funded by the Royal Society of New Zealand Marsden Fund (2012-GNS-003). Hydrological data was provided by Shaun Thomsen of Environment Canterbury, and seismic data was provided by GeoNet. Valuable feedback was provided by Helen Rutter, Chi-Yuen Wang, Xin Liao, Zeb Etheridge, Sung Soo Koh. The data supporting the conclusions of this study can be found in the supporting information.

References

Aben, F. M., Doan, M. L., Gratier, J. P. & Renard, F. (2017). Experimental postseismic recovery of fractured rocks assisted by calcite sealing. *Geophysical Research Letters*, 44(14) 7228-7238. https://doi.org/10.1002/2017GL073965

Agnew, D. C. (2005). Earth tides: An introduction. *University of California, San Diego, CA, USA.*

Agnew, D. C. (2012). SPOTL: Some Programs for Ocean-Tide Loading, *SIO Technical Report, Scripps Institution of Oceanography*

Akita, F. & Matsumoto, N. (2004). Hydrological responses induced by the Tokachi-oki earthquake in 2003 at hot spring wells in Hokkaido, Japan. *Geophysical Research Letters*. 31(16),1-4. https://doi.org/10.1029/2004GL020433

Arad, A. (1983). A summary of the artesian coastal basin of Guyana. *Journal of Hydrology*, 63, 299-313. https://doi.org/10.1016/0022-1694(83)90047-1

Bal, A. (1996). Valley fills and coastal cliffs buried beneath an alluvial plain: Evidence from variation of permeabilities in gravel aquifers, Canterbury Plains, New Zealand. *Journal of Hydrology, New Zealand*, 35(1), 1-27.

Berryman, K. R., Beanland, S., Cooper, A. F., Cutten, H. N., Norris, R. J., & Wood, P. R. (1992). The Alpine Fault, New Zealand: variation in Quarternary structural style and geomorphic expression. *Annales tectonicae*, 6, 126-163.

Boulton, C., Yao, L., Faulkner, D. R., Townend, J., Toy, V. G., Sutherland, R., et al. (2017). High-velocity frictional properties of Alpine Fault rocks: Mechanical data, microstructural analysis, and implications for rupture propagation. *Journal of Structural Geology*, 97, 71-92. https://doi.org/10.1016/j.jsg.2017.02.003

Bower, D. R. & Heaton, K. C. (1978). Response of an aquifer neat Ottawa to tidal forcing and the Alaskan earthquake of 1964. *Canadian Journal of Earth Sciences*, 15(3), 331-340. https://doi.org/10.1139/e78-039

Bredehoeft, J. D. (1967). Response of Well-Aquifer Systems to Earth Tides. *Journal of Geophysical Research*, 72(12), 3075-3087. https://doi.org/10.1029/JZ072i012p03075

Brodsky, E. E., Roeloffs, E., Woodcock, D., Gall, I., & Manga, M. (2003). A mechanism for sustained groundwater pressure changes induced by distant earthquakes. *Journal of Geophysical Research*, 108(B8), 1-10. https://doi.org/10.1029/2002JB002321

Brown, L. J. (2001). Canterbury, Groundwaters of New Zealand, New Zealand Hydrological Society. Inc., Wellington, 441-459.

Brown, L. & Weeber, J. H. (1992). Geology of the Christchurch urban area: scale 1:50,000. *Lower Hutt, GNS Science. Institute of Geological & Nuclear Sciences.*

Chen, G., Zhou, Z., Sun, T., Wu, Q., Xu, L., Khoshnevisan, S., & Ling, D. (2018). Shear Modulus and Damping Ratio of Sand–Gravel Mixtures Over a Wide Strain Range. *Journal of Earthquake Engineering*, 1-34. https://doi.org/10.1080/13632469.2017.1387200

Chia, Y., Chiu, J. J., Chiang, Y-H., Lee, T-P., Wu, Y-M., & Horng, M-J. (2008). Implications of coseismic groundwater level changes observed at multiple-well monitoring stations. *Geophysical Journal International*, 172, 293-301. https://doi.org/10.1111/j.1365-246X.2007.03628.x

Clayton, C. R. I. (2011). Stiffness at small strain: research and practice. *Géotechnique*, *61*(1), 5-37. https://doi.org/10.1680/geot.2011.61.1.5

Cox, S. C., Menzies, C. D., Sutherland, R., Denys, P. H., Chamberlain, C., & Teagle, D. A. H. (2015). Changes in hot spring temperature and hydrogeology of the Alpine Fault hanging wall, New Zealand, induced by distal South Island earthquakes. *Geofluids*, 15(1-2), 216-239. https://doi.org/10.1111/gfl.12093

Cox, S. C., Rutter, H. K., Sims, A., Manga, M., Weir, J. J., Ezzy, T., et al. (2012). Hydrological effects of the M W 7 . 1 Darfield (Canterbury) earthquake, 4 September 2010, New Zealand. *New Zealand Journal of Geology and Geophysics*, 55(3), 231-247. https://doi.org/10.1080/00288306.2012.680474

Dann, R. L., Close, M. E., Pang, L., Flintoft, M. J., & Hector, R. P. (2008). Complementary use of tracers and pumping tests to characterize a heterogeneous channelized aquifer system in New Zealand. *Hydrogeology Journal*, 16 (6), 1177-1191. https://doi.org/10.1007/s10040-008-0291-4

Dempsey, E. D., Holdsworth, R. E., Imber, J., Bistacchi, A., & Di Toro, G. (2014). A geological explanation for intraplate earthquake clustering complexity: The zeolite-bearing fault/fracture networks in the Adamello Massif (Southern Italian Alps). *Journal of Structural Geology*, 66, 58-74. https://doi.org/10.1016/j.jsg.2014.04.009

DeMets, C., Gordon, R. G., & Argus, D. F. (2010). Geologically current plate motions. *Geophysical Journal International*, 181(1), 1-80. https://doi.org/10.1111/j.1365-246X.2009.04491.x

Doan, M. L. (2005). Étude in-situ des interactions hydromécaniques entre fluides et failles. Application au Laboratoire du Rift de Corinthe. PhD thesis, Institut de Physique du Globe de Paris.

Doan, M. L., Brodsky, E. E., Prioul, R., & Signer, C. (2006). Tidal analysis of borehole pressure – A tutorial. University of California, Santa Cruz, 25, p.27.

Dobry, R., Ladd, R. S.,Yokel, F. Y., Chung, R. M., & Powell, D. (1982). Prediction of pore water pressure buildup and liquefaction of sands during earthquakes by the cyclic strain method, *National Bureau of Standards Building Science Series, 138*, National Bureau of Standards and Technology, Gaithersburg, Md., pp. 150.

Ebdon, D. (1985) *Statistics in Geography*. Blackwell.

Elkhoury, J. E., Brodsky, E. E., & Agnew, D. C. (2006). Seismic waves increase permeability. *Nature*, 441(7097), 1135-1138. https://doi.org/10.1038/nature04798

Elkhoury, J. E., Niemeijer, A., Brodsky, E. E., & Marone, C. (2011). Laboratory observations of permeability enhancement by fluid pressure oscillation of in situ fractured rock. *Journal of Geophysical Research: Solid Earth*, 116(2), 1-15. https://doi.org/10.1029/2010JB007759

Ferris, J. G. (1951). Cyclic fluctuations of water level as a basis for determining aquifer transmissibility: Internat. Geodesy Geophysics Union, Assoc. Sci. Hydrology Gen. Assembly, Brussels, 2: 148-155.

Forsyth, P.J., Barrell, D. J. A., & Jongens, R. (2008). Geology of the Christchurch area: scale 1:250,000. Lower Hutt, GNS Science. Institute of Geological & Nuclear Sciences 1:250,000 geological map 16. 67 p.+1 folded map.

Gleeson, T. & Ingebritsen, S. E. (2017). Crustal permeability. John Wiley & Sons.

Gluyas, J. & Swarbrick, R. (2013). Petroleum Geoscience. John Wiley & Sons.

Gratier, J.P. & Gueydan, F. (2007). Deformation in the presence of fluids and mineral reactions: Effect of fracturing and fluid-rock interaction on seismic cycles. *Tectonic Faults: Agents of Change on a Dynamic Earth*, 319-356.

Gulley, A. K., Dudley, N. F., Cox, S. C., & Kaipio, J. P. (2013). Groundwater responses to the recent Canterbury earthquakes: a comparison. *Journal of Hydrology*, 504, 171-181. https://doi.org/10.1016/j.jhydrol.2013.09.018

Hardin, B. O., & Drnevich, V. P. (1972). Shear modulus and damping in soils: design equations and curves. *Journal of Soil Mechanics & Foundations Div*, *98*(sm7).

Horspool, N. A., Chadwick, J., Ristau, J., Salichon, J., & Gerstenberger, M. C. (2015). ShakeMapNZ: Informing post-event decision making. *2015 NZSEE Conference*, 370-376.

Hsieh, P. A., Bredehoeft, J. D., & Farr, J. M. (1987). Determination of aquifer transmissivity from Earth tide analysis. *Water Resources Research*, 23(10), 1824-1832. https://doi.org/10.1029/WR023i010p01824

Jaeger, J., & Cook, N. (1979). Fundamentals of Rock Mechanics. 3rd ed, Chapman and Hall, London.

Jónsson, S., Segall, P., Pedersen, R., & Björnsson, G. (2003). Post-earthquake ground movements correlated to pore-pressure transients. *Nature*, 424, 179-183. https://doi.org/10.1038/nature01776

Kaiser, A., Holden, C., Beavan, J., Beetham, D., Benites, R., Celentano, A., ... & Denys, P. (2012). The Mw 6.2 Christchurch earthquake of February 2011: preliminary report. *New Zealand journal of geology and geophysics*, *55*(1), 67-90. https://doi.org/10.1080/00288306.2011.641182

Lay, T., & Wallace, T. C. (1995). Modern Global Seismology. San Diego: Academic Press, 521 pp.

Lai, G., Ge, H., Xue, L., Brodsky, E. E., Huang, F., & Wand, W. (2014). Tidal response variation and recovery following the Wenchuan earthquake from water level data of multiple wells in the nearfield. *Tectonophysics*, 619-620, 115-122. https://doi.org/10.1016/j.tecto.2013.08.039

Lees, J.J., Ballagh R.H., Orense R.P., van Ballegooy S., 2015. CPT-based analysis of liquefaction and re-liquefaction following the Canterbury earthquake sequence. *Soil Dynamics and Earthquake Engineering* ***79***, 304-314.

Liao, X., Wang, C. Y., & Liu, C. P. (2015). Disruption of groundwater system by large earthquakes. *Geophysical Research Letters*, 42, 9578-9763. https://doi.org/10.1002/2015GL066394

Liu, C., Wang, G., Shi, Z., Xu, Y., Fang, H., & Wang, J. (2013). Tide-factor anomalies from observations of well level in the Sichuan Province prior to the great Wenchuan earthquake of 2008. *Journal of Geodynamics*, 63, 54-61. https://doi.org/10.1016/j.jog.2012.09.005

Luong, M. P. (1980). Stress-strain aspects of cohesionless soils under cyclic and transient loading. In: Pnade, G. N., and Zienkiewicz (eds.), *Proc. Intern. Symp. Soils under Cyclic and Transient Loading* , p. 315-324, Rotterdam, Netherlands: A. A. Balkema.

Mair, R. J., & Wood, D. M. (2013). *Pressuremeter testing: methods and interpretation*. Elsevier.

Manga, M. & Brodsky, E. (2006). Seismic triggering of eruptions in the far field: Volcanoes and Geysers. *Annual Review of Earth and Planetary Sciences*, 34(1), 263-291. https://doi.org/10.1146/annurev.earth.35.031405,125125

Manga, M. & Wang, C.-Y. (2007). Earthquake hydrology, In: H. Kanamori (ed.), Treatise in Geophysics, G. Schubert editor: 4, 293-320.

Menzies, C. D., Teagle, D. A. H., Niedermann, S., Cox, S. C., Craw, D., Zimmer, M., et al. (2016). The fluid budget of a continental plate boundary fault: Quantification from the Alpine Fault, New Zealand. *Earth and Planetary Science Letters*, 445, 125-135. https://doi.org/10.1016/j.epsl.2016.03.046

Merritt, M. L. (2004). Estimating hydraulic properties of the Floridan aquifer system by analysis of Earth-tide, ocean-tide and barometric effects, Collier and Hendry Counties, Florida. US Department of the Interior, US Geological Survey, 2004.

Miller, M. M. & Shirzaei, M. (2015). Spatiotemporal characterization of land subsidence and uplift in Phoenix using InSAR time series and wavelet transforms. *Journal of Geophysical Research: Solid Earth*, 120(8), 5822-5842. https://doi.org/10.1002/2015JB012017

Nativ, R. & Gutierrez, G. N. (1989). Hydrogeology and hydrochemistry of cretaceous aquifers, southern high plains, U.S.A. *Journal of Hydrology*, 108, 79-109. https://doi.org/10.1016/0022-1694(89)90279-5

Norris, R. & Cooper, A. (2001). Late Quaternary slip rates and slip partitioning on the Alpine Fault, New Zealand. *Journal of Structural Geology*, 23(2-3), 507-520. https://doi.org/10.1016/S0191-8141(00)00122-X

O'Brien, G. A., Cox, S. C., & Townend, J. (2016). Spatially and temporally systematic hydrologic changes within large geoengineering landslides, Cromwell Gorge, New Zealand, induced by multiple regional earthquakes. *Journal of Geophysical Research: Solid Earth*, 121, 1-24. https://doi.org/10.1002/2016JB013418

Orense, R.P., Pender, M., Wotherspoon, L., 2012. Analysis of soil liquefaction during the recent Canterbury (New Zealand) earthquakes. *Geotechnical Engineering Journal SEAGS & AGSSEA* ***43(2)***, 8-17.

Quigley, M. C., Hughes, M. W., Bradley, B. A., van Ballegooy, S., Reid, C., Morgenroth, J., et al. (2016). The 2010-2011 Canterbury Earthquake Sequence: Environmental effects, seismic triggering thresholds and geologic legacy. *Tectonophysics*, 672-673, 228-274. https://doi.org/10.1016/j.tecto.2016.01.044

Quilty, E., & Roeloffs, E. A. (1997). Water-level changes in response to the December 20, 1994, M4.7 earthquake near Parkfield, California. *Bulletin of the Seismological Society of America*. 87 (2), 310-317.

Roberts, P. M. (2005). Laboratory observations of altered porous fluid flow behavior in Berea sandstone induced by low-frequency dynamic stress stimulation. *Acoustical Physics*, 51(S1), S140-S148. https://doi.org/10.1134/1.2133962

Roeloffs, E. A. (1996). Poroelastic techniques in the study of earthquake-related hydrologic phenomena. *Advances in Geophysics*, 37, 135-195. https://doi.org/10.1016/S0065-2687(08)60270-8

Roeloffs, E. A. (1998). Persistent water level changes in a well near Parkfield, California, due to local and distant earthquakes. *Journal of Geophysical Research*, 103 (B1), 869-889. https://doi.org/10.1029/97JB02335

Roeloffs, E.A., Sneed, M., Galloway, D.L., Sorey, M.L., Farrar, C.D., Howle, J.F., & Hughes, J. (2003). Water-level changes induced by local and distant earthquakes at Long Valley caldera, California. *Journal of Volcanology and Geothermal Research*, 127(3-4), 269–303. https://doi.org/10.1016/S0377-0273(03)00173-2

Rojstaczer, S., Wolf, S., & Michel, R. (1995). Permeability enhancement in the shallow crust as a cause of earthquake-induced hydrological changes. *Nature*, 373(6511), 237-239. https://doi.org/10.1038/373237a0

Rutter, H. K., Cox, S. C., Dudley Ward, N. F. & Weir, J. J. (2016). Aquifer permeability change caused by a near-field earthquake, Canterbury, New Zealand. *Water Resources Research*, 52(11), 8861-8878. https://doi.org/10.1002/2015WR018524

Shi, Z., & Wang, G. (2015). Sustained groundwater level changes and permeability variation in a fault zone following the 12 May 2008, M_w 7.9 Wenchuan earthquake. *Hydrological Processes*, 29(12), 2659-2667. https://doi.org/10.1002/hyp.10387

Shi, Z., Wang, G., & Liu, C. (2013). Co-Seismic Groundwater Level Changes Induced by the May 12, 2008 Wenchuan Earthquake in the Near Field. *Pure and Applied Geophysics*, 170:1773-1783. https://doi.org/10.1007/s00024-012-0606-1

Shi, Z., Wang, G., Manga, M., & Wang, C-Y. (2015a). Mechanism of co-seismic water level change following four great earthquakes – insights from co-seismic responses throughout the Chinese mainland. *Earth and Planetary Science Letters*, 430, 66-74. https://doi.org/10.1016/j.epsl.2015.08.012

Shi, Z., Wang, G., Manga, M., Wang, C. Y. (2015b). Continental-scale water-level response to a large earthquake. *Geofluids* 15, 310-320. doi.org/10.1111/gfl.12099

Shi, Z., Zhang, S., Yan, R., & Wang, G. (2018). Fault zone permeability decrease following large earthquakes in a hydrothermal system. *Geophysical Research Letters*, *45*(3), 1387-1394. https://doi.org/10.1002/2017GL075821

Sibson, R. H. (1994). Crustal stress, faulting and fluid flow. *Geological Society, London, Special Publication*, 78(1), 69-84. https://doi.org/10.1144/GSL.SP.1994.078.01.07

Talbot, J. D., Weeber, J. H., Freeman, M. C., Mason, C. R., & Wilson, D. D. (1986). The Christchurch artesian aquifers. *North Canterbury Catchment Board*, 159.

Tamura, Y. & Agnew, D. C. (2008). Baytap08 User's Manual. Scripps Institution of Oceanography, UC San Diego.

Townend, J. & Zoback, M. D. (2000). How faulting keeps the crust strong. *Geology*, 28(5), 399-402. https://doi.org/10.1130/0091-7613(2000)28<399:HFKTCS>2.0.CO;2

Van der Kamp, G. (1972). Tidal fluctuations in a confined aquifer extending under the sea. *International Geological Congress*, 24(11), 101-106.

Vucetic, M. (1994). Cyclic threshold of shear strains in soils. *Journal of Geotechnical Engineering*, 120(12), 2208-2228. https://doi.org/10.1061/(ASCE)0733-9410(1994)120:12(2208)

Wakita, H., (1975). Water wells as possible indicators of tectonic strain. *Science*, 189(4202), 553-555. https://doi.org/10.1126/science.189.4202.553

Wang, C.Y. (2007). Liquefaction beyond the Near Field. *Seismological Research Letters*, 78(5), 512-517. https://doi.org/10.1785/gssrl.78.5.512

Wang, C. Y., Cheng, L. H., Chin, C. V., & Yu, S. B. (2001). Coseismic hydrologic response of an alluvial fan to the 1999 Chi-Chi earthquake, Taiwan. *Geology*, 29(9), 831-834. https://doi.org/10.1130/0091-7613(2001)029<0831:CHROAA>2.0.CO;2

Wang, C. Y. & Chia, Y. (2008). Mechanism of water level changes during earthquakes: Near field versus intermediate field. *Geophysical Research Letters*, 35(12), 1-5. https://doi.org/10.1029/2008GL034227

Wang, C. Y., Chia, Y., Wang, P. L., & Dreger, D. (2009). Role of S waves and Love waves in coseismic permeability enhancement. *Geophysical Research Letters*, 36(9), 1-5. https://doi.org/10.1029/2009GL037330

Wang, C. Y., Liao, X., Wang, L. P., Wang, C. H., & Manga, M. (2016). Large earthquakes create vertical permeability by breaching aquitards. *Water Resources Research,* 52, 5923-5937. https://doi.org/10.1002/2016WR018893

Wang, C. Y. & Manga, M. (2010). Earthquakes and Water, volume Lecture No. Springer.

Wang, C.-Y., Wang, C. H., and Kuo, C.-H. (2004). Temporal change in groundwater level following the 1999 (Mw = 7.5) Chi-Chi earthquake, Taiwan. *Geofluids*, 5, 210-220. doi: 10.1111/j.1468-8123.2004.00082.x

Wang, H. F. (2000). Theory of linear poroelasticity: with applications to geomechanics and hydrogeology. Princeton Series in Geophysics.

Weis, P., Driesner, T., & Heinrich, C. A. (2012). Porphyry-Copper Ore Shells Form at Stable Pressure-Temperature Fronts Within Dynamic Fluid Plumes. *Science,* 33(6114), 1613-1616. https://doi.org/10.1126/science.1225009

Wilhelm, H., Zürn, W., & Wenzel, H. G. (1997). Tidal Phenomena. *Lecture Notes in Earth Sciences, Springer, Berlin, Germany.* 66.

Xue, L., Li, H.-B., Brodsky, E.E., Xu, Z.-Q., Kano, Y., Wang, H., et al. (2013). Continuous permeability measurements record healing inside the Wenchuan earthquake fault zone. *Science*, 340(6140), 1555-1559. https://doi.org/10.1126/science.1237237

Yan, R., Wang, G., & Shi, Z. (2016). Sensitivity of hydraulic properties to dynamic strain within a fault damage zone. *Journal of Hydrology*, 543, 721-728. https://doi.org/10.1016/j.jhydrol.2016.10.043

Yan, R., Woith, H., & Rongjiang, W. (2014). Groundwater level changes induced by the 2011 Tohoku earthquake in China mainland. *Geophysical Journal International*, 119(1), 533-548. https://doi.org/10.1093/gji/ggu196

Zhan, Z., Jin, B., Wei, S., & Graves, R. W. (2011). Coulomb stress change sensitivity due to variability in mainshock source models and receiving fault parameters: a case study of 2010-2011 Christchurch, New Zealand, earthquakes. *Seismological Research Letters*, 82(6), 800-814. https://doi.org /10.1785/gssrl.82.6.800

Table 1. Table of the nine M_w 5.4 or larger earthquakes that occurred between 2008 and 2015. M_w = Moment magnitude. The average distance is the average of all the individual monitoring well epicentral distances for each earthquake.

No.	Earthquake location	Epicentre (latitutde, longitude)	Time and date (NZST)| HH:MM dd/mm/yyyy	M_w	Depth (km)	Average distance (km)
1	Hastings	–39.72, 176.85	23:25 25/08/2008	5.4	32	587
2	Dusky Sound	–45.77, 166.59	21:22 15/07/2009	7.8	12	500
3	Darfield	–43.53, 172.17	04:35 04/09/2010	7.1	11	55
4	Christchurch	–43.58, 172.68	11:51 22/02/2011	6.3	5	60
5	Christchurch	–43.57, 172.74	14:12 13/06/2011	6.0	7	63
6	Christchurch	–43.52, 172.75	15:18 23/12/2011	5.9	7	64
7	Opunake	–40.05, 173.76	22:36 03/07/2012	6.2	241	430
8	Seddon	–41.60, 174.32	17:08 21/07/2013	6.6	16	291
9	Eketahuna	–40.62, 175.86	14:52 20/01/2014	6.3	34	456

Table 2. Table of the M_2 ϕ_{lag} response types that occurred as a result of the nine M_w 5.4 or larger earthquakes in the 35 tidally sensitive monitoring wells. In 90 instances, monitoring wells lacked water-level data before and/or after the earthquake of interest and no change in tidal phase behavior could be detected. In 234 cases, no earthquake-induced change in tidal phase behavior were observed.

Earthquake	Total	No data	No response	ϕ_{lag} decrease	ϕ_{lag} increase
Hastings	35	6	29	0	0
Dusky Sound	35	4	31	0	0
Darfield	35	8	25	1	1
Christchurch (Feb)	35	15	18	1	1
Christchurch (Jun)	35	14	20	1	0
Christchurch (Dec)	35	10	24	1	0
Opunake	35	12	20	3	0
Seddon	35	11	24	0	0
Eketahuna	35	9	26	0	0
Total	315	89	217	7	2

Table 3. Table of the post-seismic water-level changes that occurred as a result of the nine M_w 5.4 or larger earthquakes in the 161 monitoring wells. In 308 instances, monitoring wells lacked water-level data before and/or after the earthquake of interest, therefore, a water-level change could not be deduced. In 866 cases no earthquake-induced water-level change was observed, while a response was observed in 203 cases.

Earthquake	Total	No data	No change	Increase	Decrease
Hastings	161	55	106	0	0
Dusky Sound	161	35	98	7	21
Darfield	161	23	48	62	28
Christchurch (Feb)	161	48	75	33	5
Christchurch (Jun)	161	45	87	11	18
Christchurch (Dec)	161	34	119	4	4
Opunake	161	44	115	2	0
Seddon	161	53	101	2	5
Eketahuna	161	43	117	1	0
Total	1449	308	866	122	81

Table 4. Combination tally of tidal behavior and water-level changes that occurred in each monitoring well in response to the nine M_w 5.4 or larger earthquakes.

Tidal change behavior	Water-level change		
	No data	No change	Change
No data	82	4	2
No response	19	153	45
ϕ_{lag} decrease	1	4	2
ϕ_{lag} increase	0	0	2

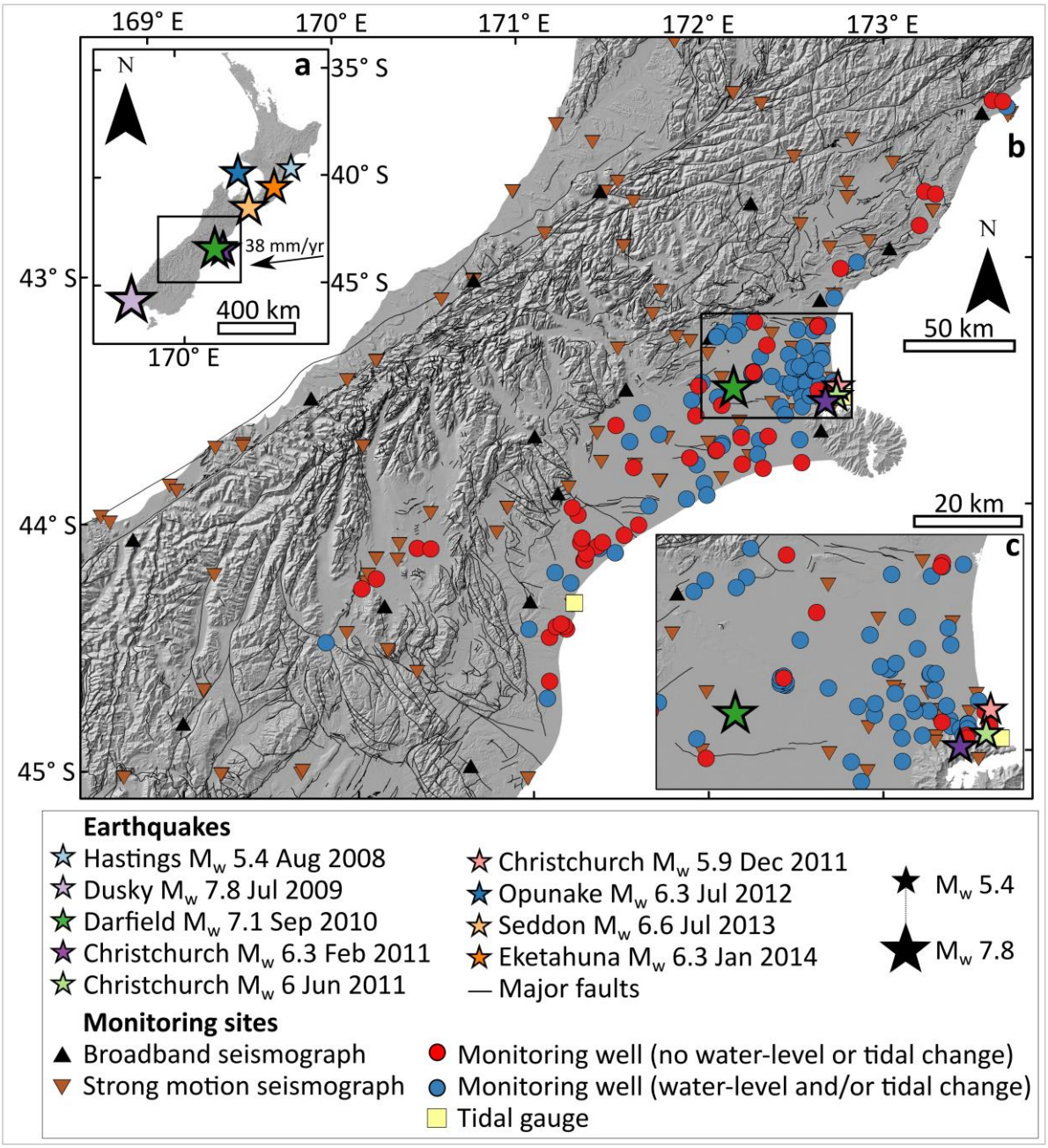

Figure 1. Seismic and hydrological monitoring in Canterbury, New Zealand. (a – Top left) Summary map showing the epicentres of the nine M_w 5.4 or larger earthquakes that occurred between 2008 and 2015. (b – Centre) Seismic and hydrological monitoring sites in the central South Island of New Zealand. (c – Bottom right) Expanded view of the Christchurch region and the four major events in 2010 and 2011 of the Canterbury earthquake sequence.

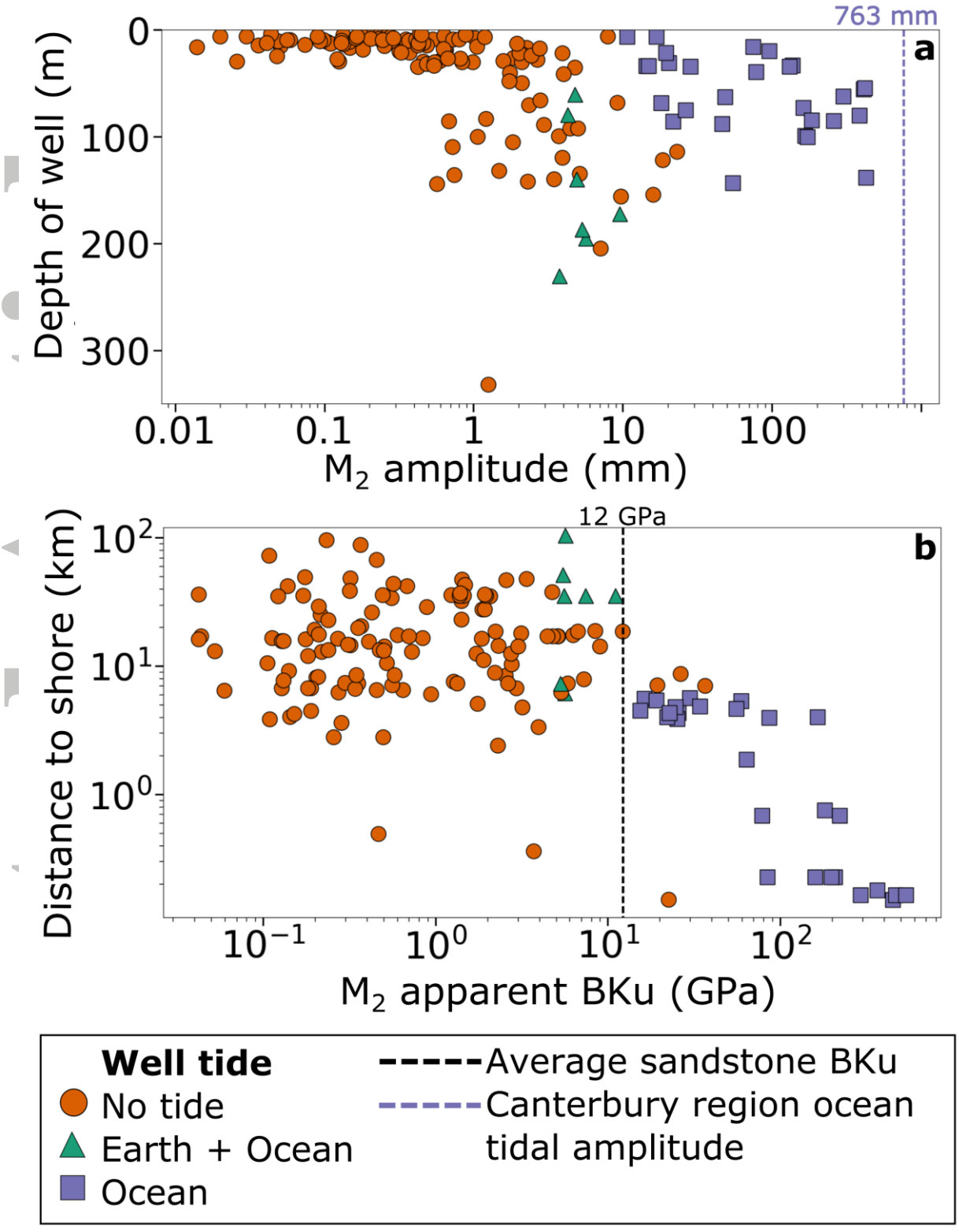

Figure 2. Monitoring well tides were characterised by the overall M_2 amplitude and BKu from 2008 to 2012. (a – Top) M_2 amplitude as a function of well depth. (b – Bottom) M_2 BKu plotted against distance to shore. The Canterbury region M_2 ocean tidal amplitude, and the arithmetic mean BKu for sandstones from Wang (2000), are included for reference.

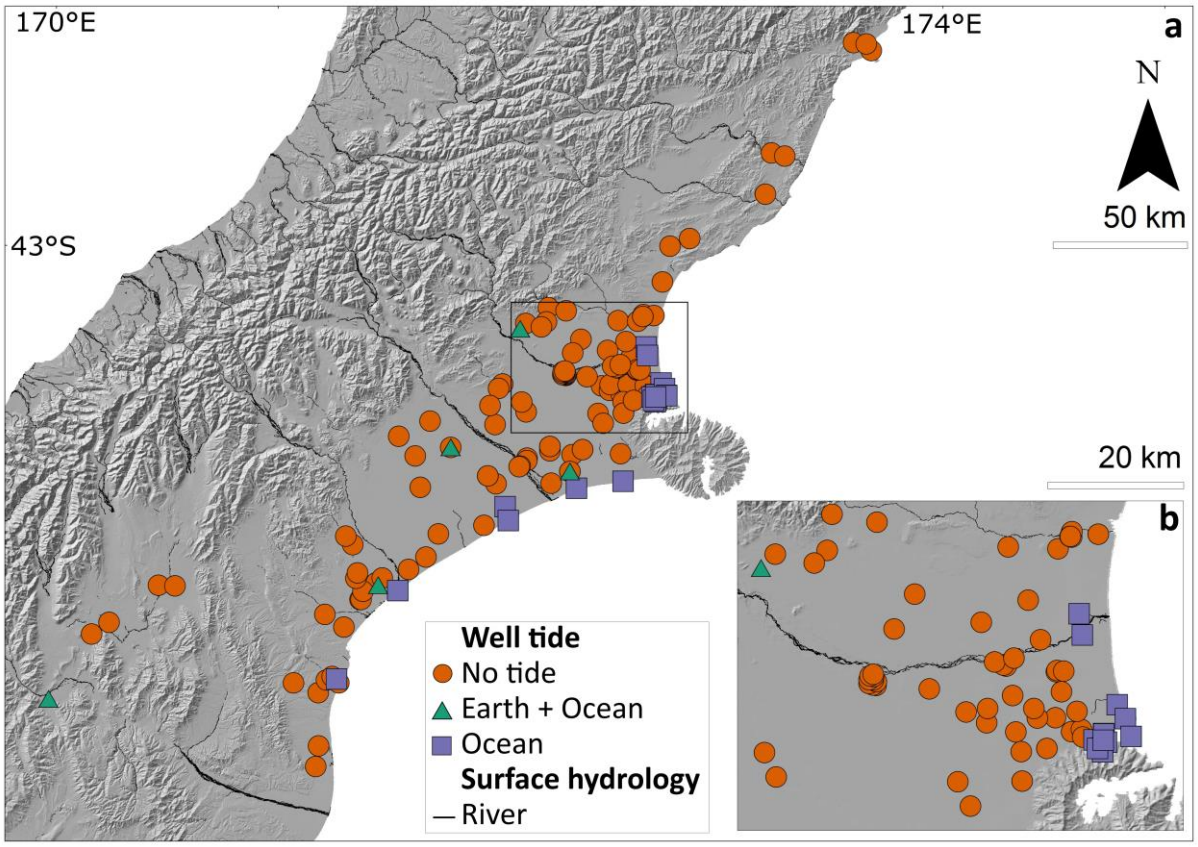

Figure 3. (A – Centre left) Distribution of monitoring wells in Canterbury, identified by the pre-dominant tide that caused water-level fluctuations. (B – Bottom Right) Expanded view of the Christchurch region. The major river networks are included for reference.

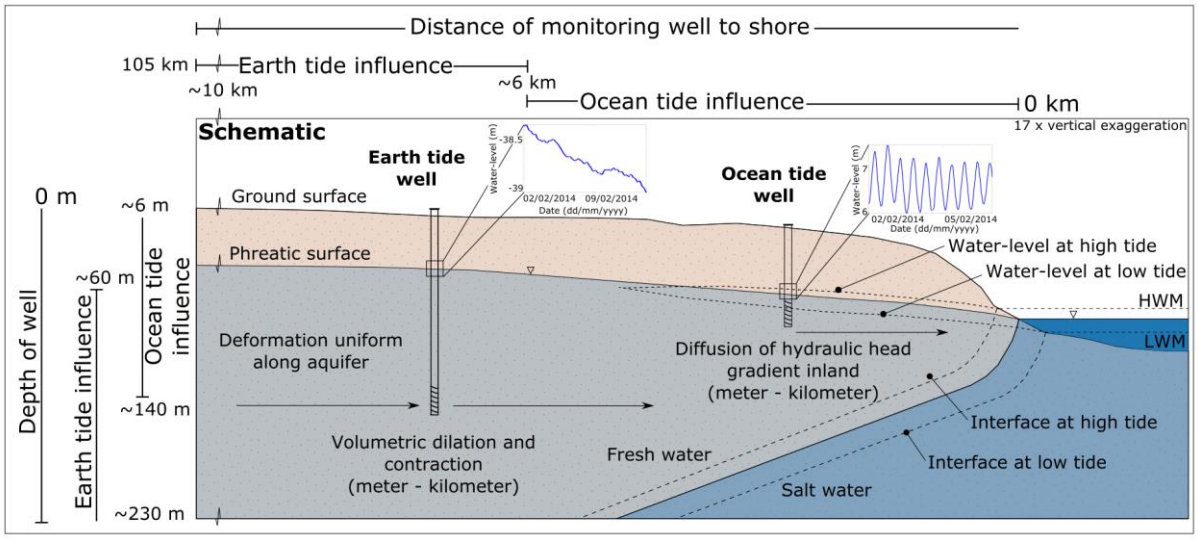

Figure 4. A schematic of the coastal Canterbury plains aquifer system. The schematic shows the zone of influence for water-level fluctuations caused by earth and ocean tides.

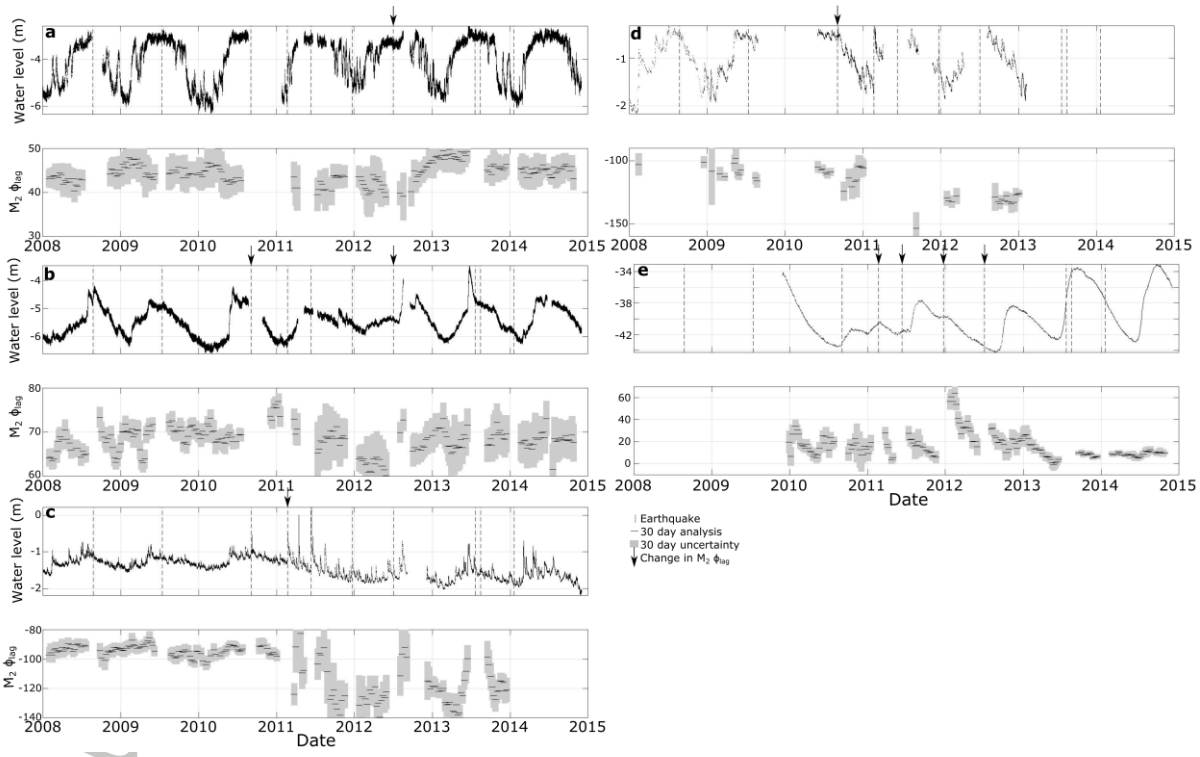

Figure 5. Water-level and M_2 ϕ_{lag} time-series for the five monitoring wells that showed a tidal change. The graphs are ordered in terms of distance from shore (a – Top left) K38/1706; (b – Middle left) K38/1821; (c – Bottom left) M36/7535; (d – Top right) M36/5384; and (e – Middle right) H39/0148. The occurrence of the nine M_w 5.4 or larger earthquakes are displayed with dashed black lines. Tidal phase behavior changes identified are highlighted in Figure 6.

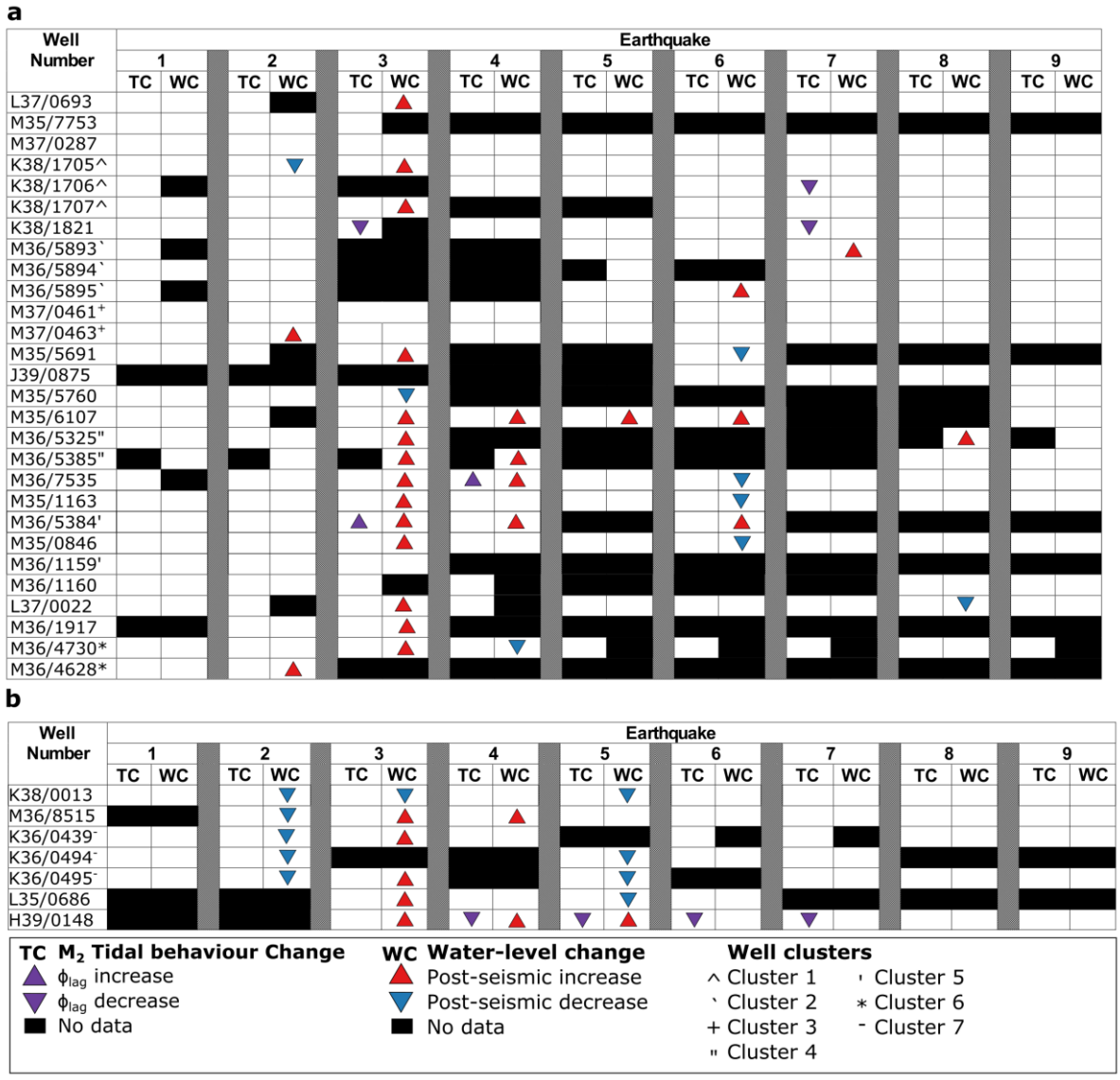

Figure 6. The tidal behavior and water-level changes that occurred in the 35 monitoring wells in response to the nine M_w 5.4 or larger earthquakes. The tables are ordered in terms of distance to shore (see Supplementary data). Well clusters represented are wells that are in very close proximity to each other (< 20 m). (a – Top) A table of the Ocean tide monitoring well response history. (b – Bottom) A table of the Earth + Ocean tide monitoring well response history. Earthquake numbers refer to Table 1.

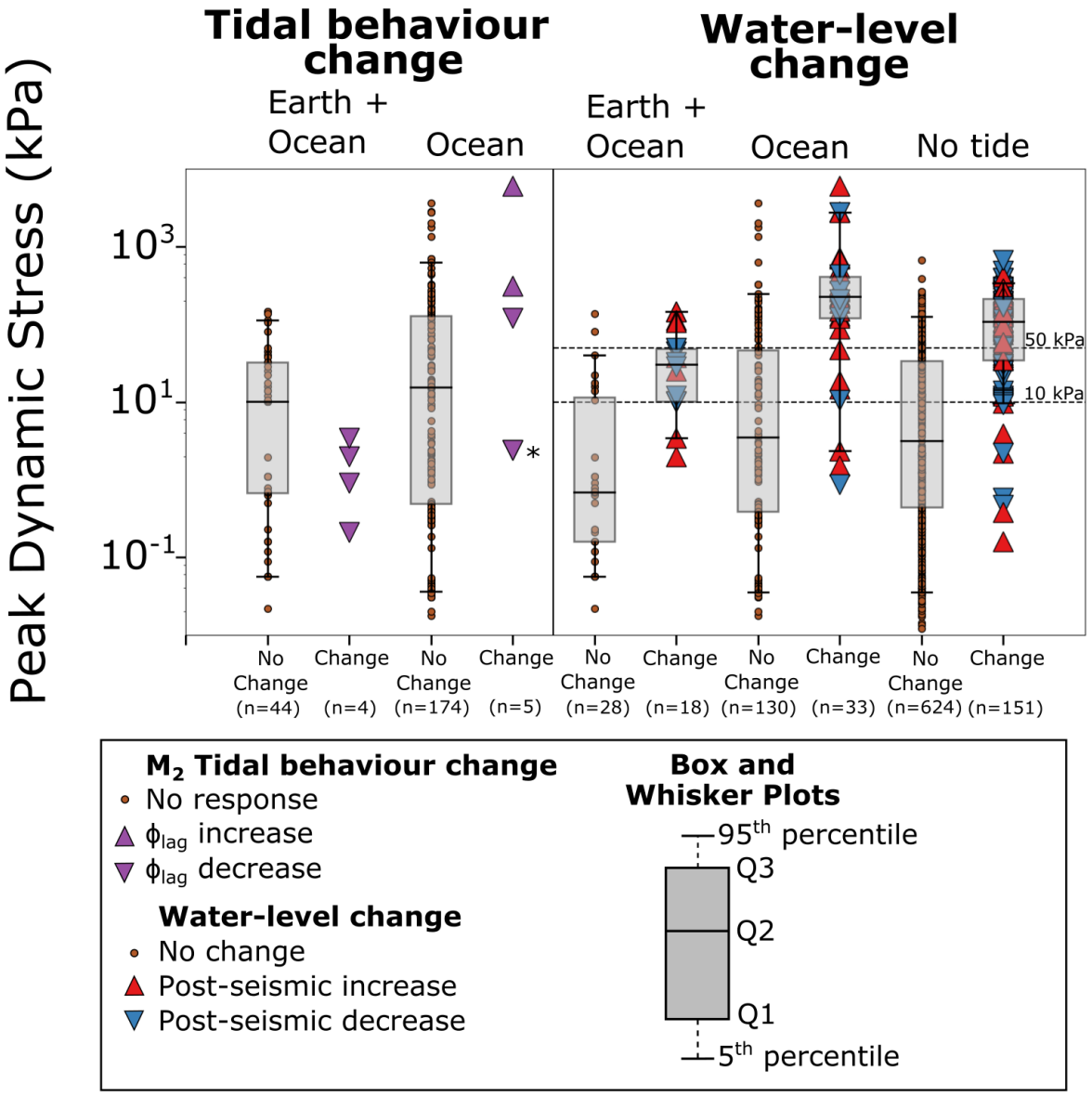

Figure 7. Interpolated peak dynamic stress produced by the nine M_w 5.4 or larger earthquakes and tidal behavior and water-level changes. * = ϕ_{lag} decreases occurred after the 2012 M_w 6.2 Opunake earthquake in two monitoring wells (K38/1821, K38/1706) that are close to each other (<3 m horizontal separation) and have identical peak dynamic stresses.

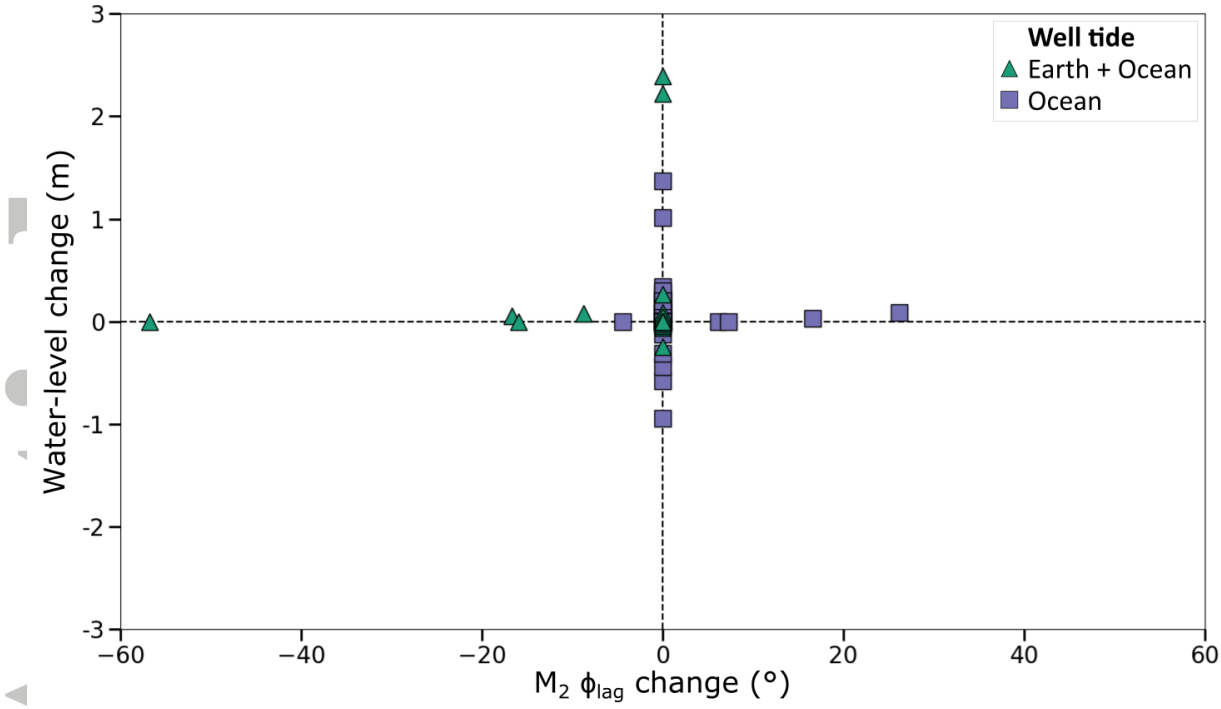

Figure 8. Cross-plots comparing water-level and M_2 ϕ_{lag} changes. Monitoring wells are distinguished by tide type. This figure illustrates that at individual sites, earthquake-induced changes in water-level were generally independent of tidal behavior changes.

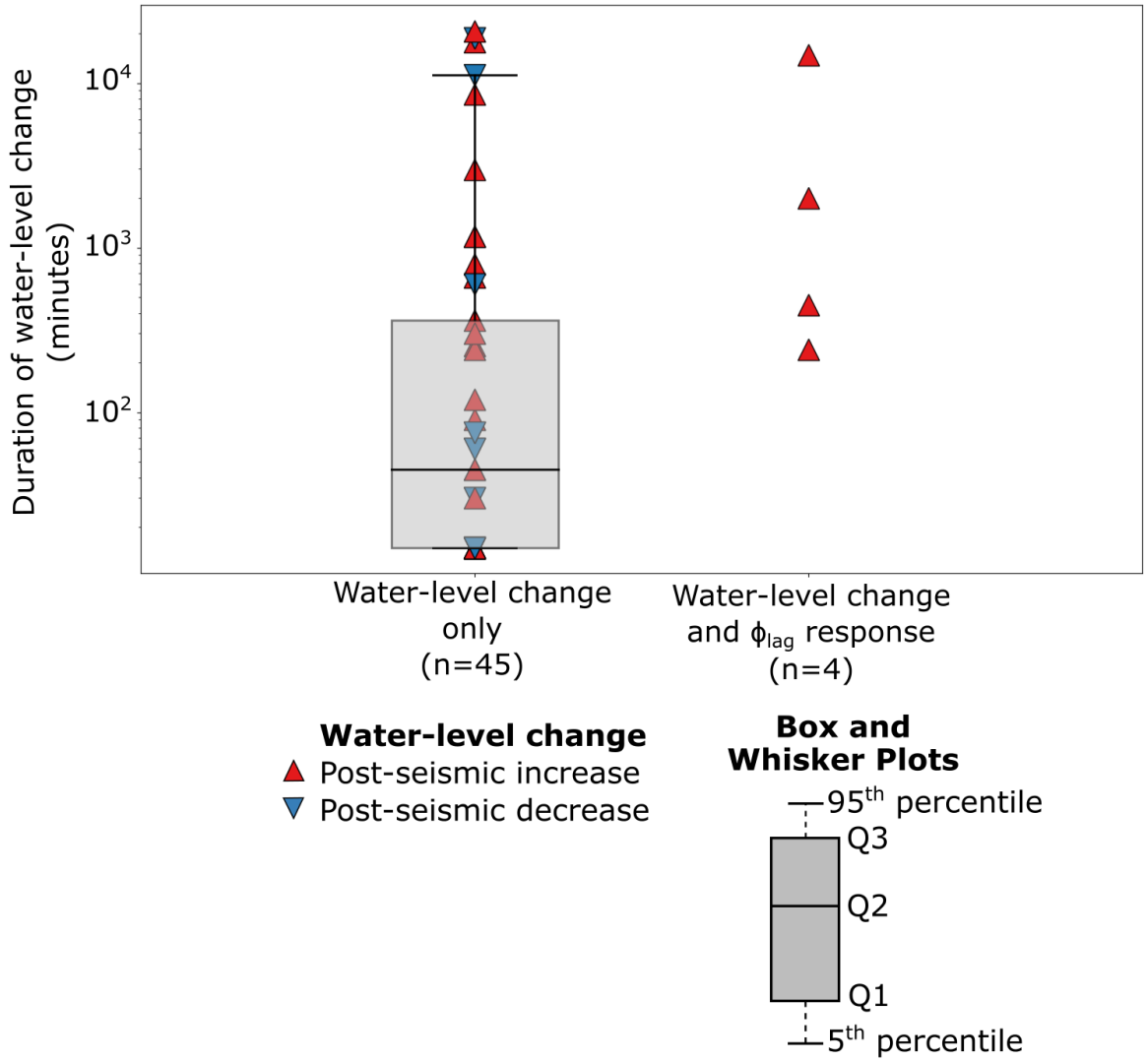

Figure 9. Box plots showing the duration of water-level changes when occurring independently and simultaneously with an M_2 ϕ_{lag} response. This figure shows that water-level changes which occur simultaneously with tidal behavior changes had generally longer durations (~240 minutes to ~10 days) than those that occurred without tidal behavior changes (~15 to 350 minutes).